SOCIAL INTERACTIONS IN PANDEMICS:
FEAR, ALTRUISM, AND RECIPROCITY

Laura Alfaro
Ester Faia
Nora Lamersdorf
Farzad Saidi

Social Interactions in Pandemics: Fear, Altruism, and Reciprocity
Laura Alfaro, Ester Faia, Nora Lamersdorf, and Farzad Saidi
NBER Working Paper No. 27134
May 2020
JEL No. D62,D64,D85,D91,I10

ABSTRACT

In SIR models, homogeneous or with a network structure, infection rates are assumed to be exogenous. However, individuals adjust their behavior. Using daily data for 89 cities worldwide, we document that mobility falls in response to fear, as approximated by Google search terms. Combining these data with experimentally validated measures of social preferences at the regional level, we find that stringency measures matter less if individuals are more patient and altruistic preference traits, and exhibit less negative reciprocity community traits. We modify the homogeneous SIR and the SIR-network model to include agents' optimizing decisions on social interactions. Susceptible individuals internalize infection risk based on their patience, infected ones do so based on their altruism, and reciprocity matters for internalizing risk in SIR networks. A planner further restricts interactions due to a static and a dynamic inefficiency in the homogeneous SIR model, and due to an additional reciprocity inefficiency in the SIR-network model. We show that partial or targeted lockdown policies are efficient only when it is possible to identify infected individuals.

Laura Alfaro
Harvard Business School
Morgan Hall 263
Soldiers Field
Boston, MA 02163
and NBER
lalfaro@hbs.edu

Ester Faia
Goethe University Frankfurt
Theodor W. Adorno Platz 3
Frankfurt am Main, 60323
Germany
and CEPR
faia@wiwi.uni-frankfurt.de

Nora Lamersdorf
Goethe University Frankfurt
Theodor W. Adorno Platz 3
Frankfurt am Main, 60323
Germany
lamersdorf@econ.uni-frankfurt.de

Farzad Saidi
Boston University
Questrom School of Business
595 Commonwealth Avenue
Boston, MA 02215
and CEPR
fsaidi@bu.edu

1. Introduction

The onset of the COVID-19 pandemic has sparked a vivid debate on policies aiming to restrict mobility, the role of heterogeneity for their effectiveness, and the potential economic cost. As such, economies considering exit strategies from lockdowns seek to implement them in a way that does not endanger a robust recovery from the public health crisis.

As the shape of the recovery is uncertain, a guiding principle for an optimal policy is to consider how the risk of disease has affected agents' behavior, which may not be uniform and could vary widely across regions and individuals. Demand spirals and excessive precautionary behavior,[1] which would impair the recovery, typically result from deep scars. The recovery is unlikely to be fast if agents maintain social-distance norms due to risk perceptions.[2] Beyond that, understanding the endogenous response of behavior to a pandemic, in particular in social interactions, can also provide further insights for forecasting how a disease spreads.

We start from the premise that fear, other-regarding preferences, and patience interact crucially with social networks in determining individuals' response to the pandemic and, in particular, their mobility. We provide evidence from international daily mobility data that fear is negatively associated with mobility at a level as granular as the city level. Furthermore, after controlling for fear, any additional effect of (typically country-wide) lockdowns or other government stringency measures on mobility varies across regions as a function of the latter's average level of patience, altruism, and reciprocity. We then rationalize these findings through the lens of the homogeneous SIR and the SIR-network model where social-activity intensity depends on individual preferences, namely patience and altruism, and on community traits, namely the matching technology's returns to scale (geographical density) and reciprocity among groups.

For our empirical analysis, we use Apple mobility data, which are obtained from GPS

---

1   A recent survey by Bartik et al. (2020) indicates that small businesses are very pessimistic about a possible recovery due to social distancing.

2   A quote from Larry Summers (Fireside Chats with Harvard Faculty on April 14, 2020) highlights this aspect: "You can open up the economy all you want, but when they're hiring refrigerator trucks to deliver dead bodies to transport them to the morgues, not many people are going to go out of their houses...so blaming the economic collapse on the policy, rather than on the problem, is fallacious in the same way that observing that wherever you see a lot of oncologists, you'll tend to see a lot of people dying of cancer and inferring that that means that oncologists kill people."
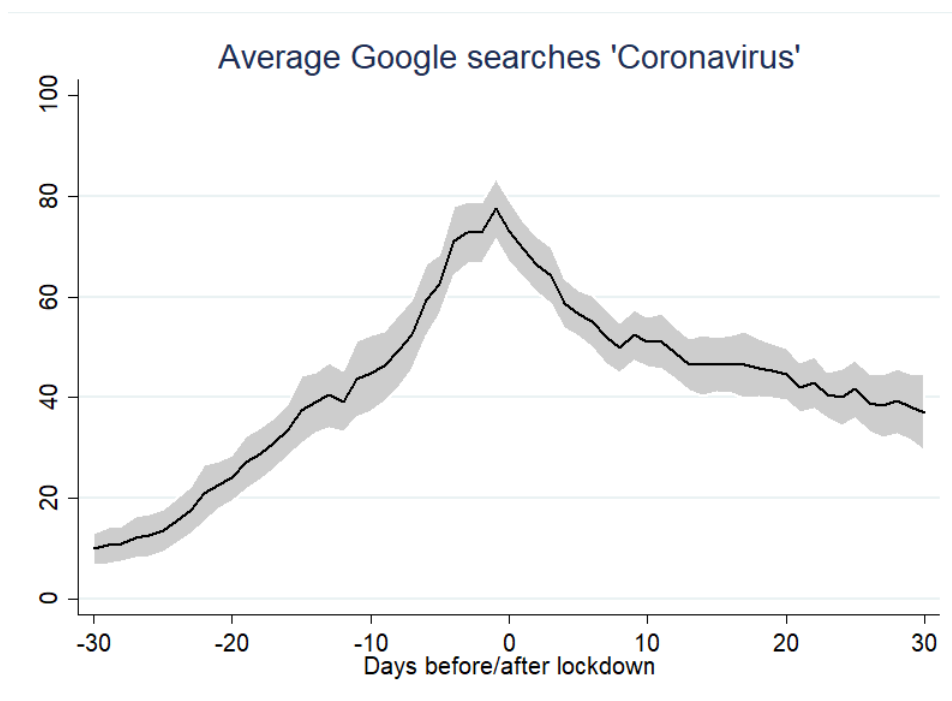
Figure 1
City-level Google Searches around Lockdown Dates across Countries

tracking. Apple Mobility data provide indicators on walking, driving and transit, and contrary to others, are daily, have the longest time coverage, and city-level granularity across 53 countries.

Figure 1 plots the average value of the Google Trends Index for "Coronavirus" in 40 countries (with lockdown dates) for the period from 30 days before to 30 days after each country's lockdown.[3] Fear, as proxied for by Google searches, increases up to shortly before the country's lockdown date, drops thereafter, and eventually levels off (around the same level as two weeks prior to the lockdown).

The negative correlation between city-level mobility and risk perceptions, or fear, is robust to controlling for lockdowns and a stringency index, both of which vary across countries (and across states in the US). Stringency policies also have a mitigating effect on mobility, but conditionally on time and social preferences, which we capture by experimentally validated survey measures from the Global Preferences Survey (see Falk et al. (2018)).

Importantly, such granular data allow us to exploit regional variation, and to test for heterogeneous effects across regions within a country following lockdowns as a function of

---

3   We use the earliest date for any state-level lockdown in the US.

average preferences in those regions. To control for time-varying unobserved heterogeneity at the country level, we incorporate country-month fixed effects. After including the latter and controlling for fear, we find that the impact of stringency policies, such as lockdowns, on mobility is muted in regions in which individuals are more patient, in which they have a higher degree of altruism, and in which they exhibit less negative reciprocity.

Motivated by these findings, we enrich an SIR model from epidemiology,[4] and in particular modify both the homogeneous SIR and the SIR-network model to account for agents' optimizing decisions on social interactions.[5] Even more modern variants of this class of models, which account for the heterogeneous topology of contact networks, assume exogenous contact rates, something starkly at odds with reality. We show that preference and community traits matter in line with our empirical evidence: susceptible individuals internalize infection risk based on their patience, infected individuals do so based based on their altruism, and reciprocity matters for internalizing risk in SIR networks.

Despite this adjustment in behaviors, a social planner might want to restrict interactions on top and above due to a static and a dynamic inefficiency. The planner internalizes the effect of individual social activities on the overall congestion of a community, which leads to the static inefficiency. The planner is also aware that her policies can affect the future number of infected, which in turn gives rise to a dynamic inefficiency.[6] We decompose the two inefficiencies, and show that they depend, among others, on the matching technology's returns to scale, which capture location density and infrastructure. In the SIR-network model, an additional inefficiency arises since the planner also internalizes the differential impact that the activity of each group has on the average infection rate of the others based on their mutual reciprocity. Finally, we show that for lockdown policies targeted towards certain groups to be efficient, one requires the ability to identify infected individuals.

Relation to Literature. While we devise an application to the pandemic, our theory belongs and contributes to the class of models used to study informal insurance in random

---

4   SIR stands for "S," the number of susceptible, "I," the number of infectious, and "R," the number of recovered, deceased, or immune individuals.

5   Recently, other papers have included some form of optimizing behavior as well. We review them below.

6   This is similar to Moser and Yared (2020), in that we highlight a dynamic inefficiency related to the social planner's commitment.

and social networks. This literature studies how transfers and obligations translate into global risk sharing (see Ambrus et al. (2014), Bloch et al. (2008), or Bramoulle and Kranton (2007)). As in those models, links, whether random or directed, have utility values, and social interactions are chosen by sharing the infection risk within a community.

Our empirical analysis contributes to a burgeoning literature that scrutinizes the development of mobility around the pandemic (see Coven and Gupta (2020) as well as Durante et al. (2020)). In contrast to these studies, we employ novel data for 89 cities worldwide in conjunction with experimentally validated survey measures that link economic preferences and community structure (e.g., through reciprocity).

The theoretical literature on the economics of pandemics is already vast. We list here some of the most important theoretical contributions we are aware of, as of today, that merge economic and SIR models. Those include Atkenson (2020), Alvarez et al. (2020), Eichenbaum et al. (2020), Kaplan et al. (2020), Krueger et al. (2020), Glover et al. (2020), and many others. Some of them note within different modeling frameworks that the activities of the agents outside of their own homes are not exogenous, but depend on optimizing decisions. In addition, many note the different incentives in internalizing the health externality faced by susceptible and infected individuals. Closer to us is Garibaldi et al. (2020), on which we build by differentiating the decision problem of the susceptible and the infected, and by introducing the optimizing choice of social interaction in SIR networks. Farboodi et al. (2020) also model the choice of social-activity intensity during a pandemic in a random search environment. Acemoglu et al. (2020) model an SIR network where contacts are determined based on a Diamond (1982) style exogenous matching function.

In the epidemiology literature, there is a large number of SIR variants (starting with Kermack and McKendrick (1927) and more recently Hethcote (2000)), all with exogenous contacts. In particular, there are SIR networks with bosonic-type reaction-diffusion processes (see, for instance, Colizza et al. (2007), Pastor-Satorras and Vespigiani (2001), and Pastor-Satorras and Vespigiani (2000)) or activity-driven SIR networks (see Moinet et al. (2018) and Perra et al. (2018), who also include a fixed risk-perception parameter that induces a decaying process in the infection rate).

2. Empirical Analysis

In the following, we first describe the data that we use in our empirical analysis. After presenting some evidence for the development of mobility around lockdowns across different cities and countries, we discuss our empirical strategy for uncovering heterogeneous effects in the effectiveness of lockdowns and the relationship between mobility and fear.

2.1. Data Description

To measure mobility at the country and city level, we use data provided by Apple, which stem from direction requests in Apple Maps.[7] Mobility is split into three categories: walking, driving, and transit. The data are at a daily frequency and start in January 2020. They cover 53 countries and 89 cities, of which 15 cities are located in 13 states across the US. Our sample period comprises three months in 2020, namely from January 22 to April 21.

To obtain an index reflecting potential fear regarding COVID-19, we use the daily number of Google searches for the term "Coronavirus" in each country and region, provided by Google Trends.[8] For a given time period (in our case, three months), Google Trends assigns to the day with the highest search volume in a given country or region the value 100, and re-scales all other days accordingly. Since this leads to large spikes in the time-series data, we use the natural logarithm of these values.

We obtain daily numbers on infections due to COVID-19 at the country level from Johns Hopkins University.[9] This time series starts on January 22, 2020, which sets the beginning of the time span covered in our empirical analysis. To capture policy responses of governments across the globe, we take two approaches. First, we generate a dummy variable that is one from the first day of an official country-wide (or state-wide) lockdown onward, and zero otherwise. For this purpose, we use the lockdown dates provided by Wikipedia.[10] Since in the US, the adopted policy responses may differ across states, we use the state-wide lockdown dates for a given city in that state for our city-level regressions.

---

7   See https://www.apple.com/covid19/mobility.

8   See https://trends.google.com/trends/?geo=US.

9   See https://github.com/CSSEGISandData/COVID-19/tree/master/csse_covid_19_data/csse_covid_19_time_series.

10 See https://en.wikipedia.org/wiki/Curfews_and_lockdowns_related_to_the_2019%E2%80%9320_coronavirus_pandemic.

Relatedly, lockdown measures may also vary widely across countries. For this reason, we use as an alternative measure the so-called stringency index, between 0 and 100, at the country-day level from the Oxford COVID-19 Government Response Tracker (OxCGRT), which is available from January, 1, 2020 onward. This index combines several different policy responses governments have taken, and aggregates them into a single measure that is comparable across countries.[11]

To analyze whether the effect of government responses on mobility depends on country- or region-specific economic preferences, we use a set of variables from the Global Preferences Survey.[12] This globally representative dataset includes responses regarding time, risk, and social preferences for a large number (80,000) of individuals for all countries in our sample. In particular, this dataset provides us with experimentally validated measures of altruism, patience, and negative reciprocity. These variables map to parameters of our theoretical model and, thus, enable us to test for heterogeneous effects in our empirical analysis.

As pointed out by Falk et al. (2018), economic preferences tend to differ significantly within countries. Therefore, we use their dataset on individual, rather than country-level, survey responses, and compute for each variable the average value at the level of the regions corresponding to the cities included in the Apple Mobility data.

We present summary statistics in Table 1. In particular, the statistics in the first four columns pertain to the country-day level ct, whereas those in the last four columns are at the more granular city-day level it for the mobility outcomes, and at the region-day level gt for all remaining variables. Mirroring our regression sample in the respective tables, the sample in the last four columns is furthermore limited to countries with at least two cities in different regions. In this manner, we are left with 60, of which 15 are in the US, out of our total of 89 cities.

All three mobility indices exhibit similar average values both at the country and at the city level, with (mechanically) smaller variations at the more aggregate country level. The

---

11 For more information and the current version of a working paper describing the approach, see https://www.bsg.ox.ac.uk/research/research-projects/coronavirus-government-response-tracker.

12 For more information on this survey, see https://www.briq-institute.org/global-preferences/home and also Falk et al. (2016, 2018).
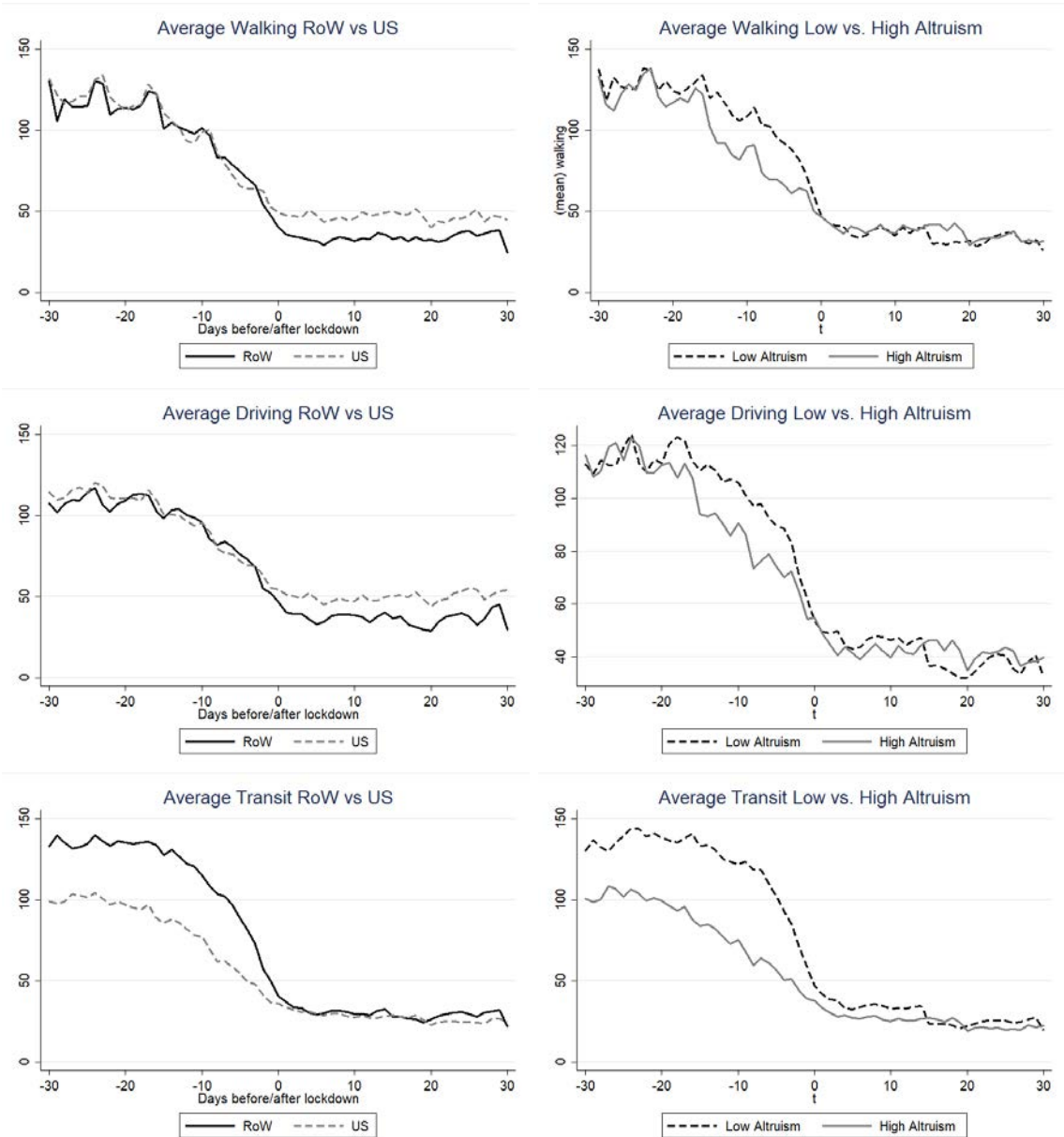
Figure 2
Mobility around Global Lockdown Dates

same holds true for the the Google Trends Index for the search term "Coronavirus" at the country and regional levels. Finally, we include summary statistics for the three variables from the Global Preferences Survey (Falk et al. (2018)), which are available at the regional level. While altruism and patience are positively correlated (with a correlation coefficient of 0.24), both are negatively correlated with the proxy for negative reciprocity (-0.15 and -0.10).

2.2. Motivating Evidence

We start by presenting evidence that motivates our investigation of the effect of fear on mobility, and the role of other-regarding preferences for the effectiveness of lockdowns. In Figure 2, we plot average city-level values for the walking, driving, and transit indices, based on the Apple Mobility data, around lockdown dates (in our regression sample limited to countries with at least two cities in different regions), which are determined at the state level in the US and at the country level in all other countries. The three figures in the left panel plot these time series for the US vs. the rest of the world (RoW), and the three figures in the right panel plot these time series for regions in which individuals report to exhibit different average levels of altruism (based on the Global Preferences Survey).

The following stylized facts emerge. In the left panel of Figure 2, mobility is drastically reduced well in advance of any lockdown, drops more outside of the US, but stabilizes both in the US and elsewhere during the post-lockdown month. In the right panel, the pre-lockdown reduction in mobility is more emphasized in regions in which individuals have other-regarding preferences, which we approximate by sorting regions into the top vs. bottom quarter in terms of $Altruism_g$.

We next discuss our empirical strategy for formally testing these relationships in a regression framework.

2.3. Empirical Specification

To assess the relationship between government responses and mobility across different cities worldwide, controlling for fear, we estimate the following regression specification at the city-day level it, with each city i being located in region g of country c:

$$\ln(Mobility)_{it} = \beta_1 \ln(Corona\ ST)_{ct-1} + \beta_2 Lockdown_{ct} + \beta_3 \mathbf{X}_{ct} + \mu_i + \delta_t + \epsilon_{it}, \quad (1)$$

where the dependent variable is the natural logarithm of Apple Mobility's walking, driving, or transit index for city i at date t; $Corona\ ST_{ct-1}$ is the Google Trends Index for the search

term "Coronavirus" in country c at date $t-1$; $Lockdown_{ct}$ is an indicator variable for the lockdown period in country c (or state/region g for the US) at date t; $\mathbf{X}_{ct}$ denotes control variables at the country-day level; and μ_i and δ_t denote city and day fixed effects, respectively. Standard errors are (conservatively) double-clustered at the city and day levels.

In contrasting between fear, as captured by β_1, and government (typically country-level) responses, as captured by β_2, we can further refine our measure of the former by using the regional average of the Google Trends Index for "Coronavirus." This effectively enables us to exploit variation in fear across different regions in the same country, in which all regions typically face the same lockdown measures (the US is the only notable exception in our data).

For this reason, when we use regional variation in $Corona\ ST_{gt}$, we limit the sample to countries c with at least two cities i in different regions g. This, in turn, allows us to include country-month fixed effects, thereby estimating the effect of lockdowns, or other government measures, while holding constant all remaining sources of unobserved heterogeneity at the country level in a given month. In this setting, we can then test for heterogeneous effects across regions within a country. In particular, we hypothesize that regions with a certain preference, $Preference_g$, such as greater altruism (see right panel of Figure 2), reduce their mobility more preceding any government responses, thereby muting any additional effect of $Lockdown_{ct}$ on mobility. To test this, we estimate the following regression specification:

$$
\begin{aligned}
\ln(Mobility)_{it} \;=\;\; & \beta_1 \ln(Corona\ ST)_{gt-1} + \beta_2 Lockdown_{ct} + \beta_3 Lockdown_{ct} \times Preference_g \\
& + \beta_4 \mathbf{X}_{ct} + \mu_i + \delta_t + \theta_{cm(t)} + \epsilon_{it},
\end{aligned} \tag{2}
$$

where $Corona\ ST_{gt-1}$ is the Google Trends Index for the search term "Coronavirus" in region g at date $t-1$; $Preference_g$ is the average value of altruism, patience, or negative reciprocity in region g (as reported by Falk et al. (2018)); and $\theta_{cm(t)}$ denotes country-month fixed effects ($m(t)$ is the month for a given day t).

Finally, by testing for the heterogeneous effect of, for instance, altruism at the regional level following lockdowns within countries, we mitigate the risk of picking up potential reverse

causality. This is because government policies are typically put in place with the entire, or rather average, population in mind.

2.4. Results

We next turn to the results. In the first three columns of Table 2, we estimate (1), and use as dependent variables the Apple mobility indices for walking, driving, and transit (the latter variable being available only for a subset of our regression sample). In addition, we control for the lagged number of infection cases in a given country. Importantly, we use country-level variation in $Corona\ ST_{ct}$, and see that fear, as proxied for by the latter variable, is negatively associated with mobility, above and beyond any government responses. In fact, the coefficient on $Lockdown_{ct}$, while negative, is not statistically significant for transit (column 3). However, this may be due to the fact that government responses are not uniform, and a simple dummy variable may mask important underlying heterogeneity.

To account for this, we replace $Lockdown_{ct}$ by $Stringency\ index_{ct}$, which is an index $\in [0, 100]$ (taken from the Oxford COVID-19 Government Response Tracker) reflecting the different policy responses that governments have taken. The estimates on the respective coefficient in the last three columns are statistically significant at the 1% level throughout, of similar or even larger size (once one accounts for the index being defined on the interval from 0 to 100) as the corresponding coefficients on $Lockdown_{ct}$, and appear to partially explain some of the effect of fear. As a consequence, the estimated coefficients on $\ln(Corona\ ST)_{ct-1}$ are somewhat smaller than in the first three columns, and the estimate in the last column becomes insignificant.

These insights hold up to using regional variation in $Corona\ ST_{gt}$ in Table 3. At least for walking and driving, fear has a robust negative association with mobility that extends beyond any government response, irrespective of how the latter is measured. The effect of fear is not only statistically but also economically significant. As can be seen in Figure 1, Google searches for "Coronavirus" have rapidly increased during the run-up period to a lockdown. For instance, observing a 25% increase in the respective Google Trends index would not be

11

out of the ordinary, which would, in turn, be associated with at least $25\% \times 0.109 = 2.7\%$ and $25\% \times 0.120 = 3.0\%$ less walking and driving, respectively, in cities (see columns 4 and 5).

We then turn to testing for heterogeneous effects across regions within a country, as a function of average preferences in said regions. In particular, we hypothesize that regions in which individuals report to be more patient should exhibit a muted response to any government measures, in particular lockdowns, as patient agents are more likely to postpone any acts of mobility for the sake of internalizing any externalities on susceptible agents. Similarly, we would expect agents with other-regarding preferences, especially altruistic agents, to behave this way. Finally, agents that exhibit negative reciprocity are more prone to mimic any acts of mobility out of inequity aversion, so the effect of government responses on reduced city-level mobility should be more emphasized for regions in which individuals exhibit greater negative reciprocity.

These preference parameters are captured by the respective variables from the Global Preferences Survey and incorporated in regression specification (2). In Tables 4, 5, and 6, we use, respectively, interactions of $Lockdown_{ct}$ with $Patience_g$, $Neg.\ reciprocity_g$, and $Altruism_g$.

We find that in regions which exhibit greater patience, the effect of lockdowns and other government responses, as captured by the stringency index, on mobility is reduced significantly, and at times undone, across the board (see Table 4).

Consistent with the idea that individuals that exhibit greater negative reciprocity are less prone to internalize externalities by reducing their mobility, we find that lockdowns are effective in imposing such behavior: the coefficient on $Lockdown_{ct} \times Neg.\ reciprocity_g$ is negative and significant for walking, driving, and transit (see columns 1 to 3 in Table 5). The respective results are qualitatively similar but weaker in terms of economic and statistical significance when replacing $Lockdown_{ct}$ by $Stringency\ index_{ct}$ (in columns 4 to 6).

Finally, the effect of lockdowns on mobility is entirely neutralized in more altruistic regions (see columns 1 to 3 in Table 6). This is in line with altruistic agents' willingness to internalize externalities on susceptible agents by reducing their mobility. As a consequence, lockdowns

do not have any effect on mobility above and beyond fear, the influence of which we capture through *Corona ST*_{gt−1}.

The results are similar but weaker after replacing lockdowns by the stringency index. However, in the last three columns of Table 6, the sum of the coefficients on *Stringency index*$_{ct}$ and *Stringency index*$_{ct}$ × *Altruism*$_g$ is not significantly different from zero for walking, driving, and transit (the respective *p*-values are 0.85, 0.33, and 0.78). This suggests that the additional impact of stringency policies may be muted for altruistic agents.

3. Limitations of SIR and SIR-Network Models

Motivated by our empirical findings, we formulate an SIR model that accounts for agents' optimizing behavior with respect to the intensity of their social activity. In the basic homogeneous SIR model (see Kermack and McKendrick (1927) or Hethcote (2000) more recently), there are three groups of agents: susceptible (S), infected (I), and recovered (R). The number of susceptible decreases as they are infected. At the same time, the number of infected increases by the same amount, but also declines because people recover. Recovered people are immune to the disease and, hence, stay recovered. The mathematical representation of the model is as follows:

$$S_{t+1} = S_t - \lambda_t I_t S_t \tag{3}$$

$$I_{t+1} = I_t + \lambda_t I_t S_t - \gamma I_t \tag{4}$$

$$R_{t+1} = R_t + \gamma I_t, \tag{5}$$

where $N = S_t + I_t + R_t$ and λ_t is the transmission rate of the infection.

Hence, $p_t = \lambda_t I_t$ is the probability that a susceptible individual is infected at time t. In the classic model, the latter is assumed to be exogenous, constant, and homogeneous across groups. Even as agents become aware of the pandemic, it is assumed that they do not adjust their behavior. More recent versions of the SIR model include the dependence of the contact rates on the heterogeneous topology of the network of contacts and mobility of

people across locations (see Colizza et al. (2007), Pastor-Satorras and Vespigiani (2001), and Pastor-Satorras and Vespigiani (2000) that include bosonic-type reaction-diffusion processes in SIR models) or the dependence of the infection rate on the activity intensity of each node of the network (see Perra et al. (2018) for solving activity-driven SIR using mean-field theory and Moinet et al. (2018) who also introduce a parameter capturing an exogenous decay of the infection risk due to precautionary behavior).

In what follows, we modify the homogeneous SIR and the SIR-network model so as to take into account how agents adjust their social-activity intensity in response to health risk and how, in turn, their equilibrium choices affect the infection rates.

4. A Model of Decision-Theory Based Social Interactions for Pandemics

We develop SIR models, both homogeneous and with a network structure, where the contact rate results from a decision problem on the extent of social interactions. Combining search and optimizing behavior in economics goes back to Diamond (1982).[13] We build on Garibaldi et al. (2020), who introduce in the homogeneous SIR model with random contacts the optimal choice of social-activity intensity.

Two major extensions are considered here. First, we distinguish the optimization problem of the susceptible, the infected, and the recovered individuals, where the susceptible internalize the health risk only under altruistic preferences.[14] Distinguishing among different maximization problems implicitly amounts to assuming that individuals know or recognize if they are infected. In the COVID-19 pandemic, a third group of individuals has emerged, namely the asymptomatic. We do not include them in our model, but the setup can be extended accordingly. The presence of different decision processes also requires a modification of the matching function. Second, we introduce an optimal choice of social-activity intensity

---

13 See Petrongolo and Pissarides (2001) for a survey.
14 See Eichenbaum et al. (2020) for the role of health externalities in a SIR-macro model.

in an SIR model with a network structure. The latter will allow us to examine the effect of reciprocity among different interconnected groups.

We start with the homogeneous SIR model where all agents in the population are the same except that they are susceptible, infected, or recovered. We label the health status with the index $i \in \{S, I, R\}$. Transitions of susceptible individuals from state S to I depend on contacts with other people,[15] and those in turn depend on the social-activity intensity of each individual in the population and on a matching technology.[16] The model is in discrete time, time goes up to the infinite horizon, and there is no aggregate or idiosyncratic uncertainty.

Each agent has a per-period utility function $U_t^i(x_{h,t}^i, x_{s,t}^i) = u^i(x_{h,t}^i, x_{s,t}^i) - c^i(x_{h,t}^i, x_{s,t}^i)$ where x_h^i denotes home activities and x_s^i denotes social activities. The function $u^i(x_h^i, x_s^i)$ has standard concavity properties and $u^i(x_h^i, 0) > 0$. The cost, $c^i(x_h^i, x_s^i)$, puts a constraint on the choice between home and social activities. At time t, a susceptible agent enjoys the per-period utility, expects to enter the infected state with probability p_t or to remain susceptible with probability $(1 - p_t)$, and chooses the amount of home and social activities by recognizing that the latter affects the risk of infection. The value function of a susceptible individual is as follows:

$$V_t^S = U(x_{h,t}^S, x_{s,t}^S) + \beta[p_t V_{t+1}^I + (1 - p_t)V_{t+1}^S], \tag{6}$$

where β is the time discount factor and p_t is the probability of being infected. The latter depends on the amount of social activity of the susceptible and infected agents, on the average amount of social activity, $\bar{x}_{s,t}$, in the population, as well as on the individual shares of each agent i in the population:

$$p_t = p_t(x_{s,t}^S, x_{s,t}^I, \bar{x}_{s,t}, \eta, S_t, I_t, R_t), \tag{7}$$

where

$$\bar{x}_{s,t} = \bar{x}_{s,t}^S \frac{S_t}{N_t} + \bar{x}_{s,t}^I \frac{I_t}{N_t}. \tag{8}$$

---

15 These can arise in entertainment activities, other activities outside of home, or at the workplace.
16 Transitions for individuals in the infected group I to recovery R depend only on medical conditions related to the disease (mostly the health system) that are outside of individuals' control.

To map the endogenous SIR model into the standard SIR model in (3) to (5), we use the convention that $p_t = \lambda_t I_t$. We will be more precise on the exact functional form of p_t later on. For now, it suffices to assume that $\frac{\partial p_t(.)}{\partial x_{s,t}^S} > 0$ and $p_t(0, .) = 0$.

In the baseline model, infected individuals do not have any altruistic motive. Their Bellman equation is:

$$V_t^I = U(x_{h,t}^I, x_{s,t}^I) + \beta[(1-\gamma)V_{t+1}^I + \gamma V_{t+1}^R]. \tag{9}$$

Currently infected individuals will remain infected for an additional period with probability $(1-\gamma)$ or will recover with probability γ. The value function of the recovered reads as follows:

$$V_t^R = U(x_{h,t}^R, x_{s,t}^R) + \beta V_{t+1}^R. \tag{10}$$

Susceptible individuals' first-order conditions with respect to $x_{h,t}$ and $x_{s,t}$ are as follows:

$$\frac{\partial U(x_{h,t}^S, x_{s,t}^S)}{\partial x_{h,t}^S} = 0 \tag{11}$$

$$\frac{\partial U(x_{h,t}^S, x_{s,t}^S)}{\partial x_{s,t}^S} + \beta \frac{\partial p_t(.)}{\partial x_{s,t}^S}(V_{t+1}^I - V_{t+1}^S) = 0, \tag{12}$$

where it is reasonable to assume that $(V_{t+1}^I - V_{t+1}^S) < 0$.

Susceptible individuals internalize the drop in utility associated with the risk of infection caused by the social activity, and choose a level of social activity which is lower than the one that they would choose in the absence of a pandemic. This parallels the empirical findings in that agents naturally reduce their mobility in response to increased fear of infection. Also, individuals reduce social interactions by more when the discount factor, i.e., β, is higher. This mirrors our empirical result that the degree of patience reduces mobility and makes the lockdown policy less effective or less needed.

The first-order conditions of the infected with respect to $x_{h,t}$ and $x_{s,t}$ read as follows:

$$\frac{\partial U(x_{h,t}^I, x_{s,t}^I)}{\partial x_{h,t}^I} = 0, \frac{\partial U(x_{h,t}^I, x_{s,t}^I)}{\partial x_{s,t}^I} = 0. \tag{13}$$

Infected individuals choose a higher level of social activity than susceptible ones since they

do not internalize the effect of their decision on the risk of infection. However, their level of social activity will in turn affect the overall infection rate. In Section 4.1, infected individuals are assumed to hold altruistic preferences. This will induce them to also internalize the effect of their actions on the infection rate of the susceptible.

Last, the first-order conditions of the recovered individuals read as follows:

$$\frac{\partial U(x_{h,t}^R, x_{s,t}^R)}{\partial x_{h,t}^R} = 0, \frac{\partial U(x_{h,t}^R, x_{s,t}^R)}{\partial x_{s,t}^R} = 0. \tag{14}$$

Recovered people choose the same level of social activity as they would in the absence of a pandemic. Given the optimal choice of social-activity intensity, we can now derive the equilibrium infection probability in the decentralized equilibrium. This involves defining a matching function (see Diamond (1982) or Pissarides (2000)). The intensity of social interaction, x_s, corresponds to the number of times people leave their home or, differently speaking, the probability per unit of time of leaving home. In each of these outside activities, individuals come in contact with other individuals. How many contacts the susceptible individuals have with the infected individuals depends on the average amount of social activity of the two. The latter is given by $\bar{x}_{s,t} = S_t \bar{x}_{s,t}^S + I_t \bar{x}_{s,t}^I$, where we have normalized the total population N to one.

It will be convenient for the derivatives later on to specify a matching function in terms of the average level of social activity of the infected and the susceptible individuals separately, $m(\bar{x}_{s,t}^S, \bar{x}_{s,t}^I)$. The matching technology's returns to scale determine the total number of contacts per average social activity. The average number of contacts between a susceptible and an infected person is given by the total number of contacts m times outside activities by infected individuals divided by the average number of outings of both susceptible and infected individuals, which is the product of the average frequency of outings of susceptible individuals, $\bar{x}_{s,t}^S$, and the average frequency of outings of infected individuals, $\bar{x}_{s,t}^S$. Hence, the average number of contacts per outside activity of an infected person is $\frac{m(\bar{x}_{s,t}^S, \bar{x}_{s,t}^I)}{\bar{x}_{s,t}^S \bar{x}_{s,t}^I}$. Finally, the probability of becoming infected depends on the probability that susceptible individuals

go out, $x_{s,t}^s$, the probability that infected individuals go out, $x_{s,t}^I$, the average number of contacts, the transmission rate, η, and the number of infected. As such, it is equal to:

$$p_t = \eta x_{s,t}^S x_{s,t}^I \frac{m(\bar{x}_{s,t}^S, \bar{x}_{s,t}^I)}{\bar{x}_{s,t}^S \bar{x}_{s,t}^I} I_t. \tag{15}$$

Note that atomistic agents take the fraction of outside activities of other agents as given. One could incorporate increasing returns to scale for the matching function as $(m(\bar{x}_{s,t}^S, \bar{x}_{s,t}^I))^\alpha$ with $\alpha > 1$. This alternative specification could be suitable, for example, when community density or topology induces a larger than proportional number of contacts per outside activity.

Given the equations above, the baseline SIR model can now be re-written as follows:

$$S_{t+1} = S_t - \eta x_{s,t}^S x_{s,t}^I \frac{m(\bar{x}_{s,t}^S, \bar{x}_{s,t}^I)}{\bar{x}_{s,t}^S \bar{x}_{s,t}^I} I_t S_t \tag{16}$$

$$I_{t+1} = I_t + \eta x_{s,t}^S x_{s,t}^I \frac{m(\bar{x}_{s,t}^S, \bar{x}_{s,t}^I)}{\bar{x}_{s,t}^S \bar{x}_{s,t}^I} I_t S_t - \gamma I_t \tag{17}$$

$$R_{t+1} = R_t + \gamma I_t, \tag{18}$$

where $S_t + I_t + R_t \equiv 1$.

Definition 1. A decentralized equilibrium is a sequence of state variables, S_t, I_t, R_t, a set of value functions, V_t^S, V_t^I, V_t^R, and a sequence of consumption, probabilities, and social contacts, $p_t, x_{h,t}^S, x_{h,t}^I, x_{h,t}^R, x_{s,t}^S, x_{s,t}^I, x_{s,t}^R$, such that:

1. S_t, I_t, R_t solve (3) to (5), with the probability of contact given by (15)

2. V_t^S, V_t^I, V_t^R solve (6), (9), and (10)

3. The sequence $p_t, x_{h,t}^S, x_{h,t}^I, x_{h,t}^R, x_{s,t}^S, x_{s,t}^I, x_{s,t}^R$ solves (11), (12), (13), and (14).

4.1. Altruism of Infected Individuals

Our empirical results have highlighted that the degree of altruism matters. It is also reasonable to conjecture that infected individuals hold some altruistic preferences. These attitudes may

include both warm-glow preferences toward relatives and friends (see Becker (1974))[17] or general unconditional altruism and social preferences.[18] For this reason, we now extend their per-period utility to include some altruistic preferences. Their per-period utility is now defined as follows:

$$U(x_{h,t}^I, x_{s,t}^I) = u(x_{h,t}^I, x_{s,t}^I) - c(x_{h,t}^I, x_{s,t}^I) + \delta V_t^S. \tag{19}$$

While infected individuals do not internalize the effect of their social activities on the infection rate fully, as they are already immune in the near future, they do hold an altruistic motive toward the susceptible, which is captured by a weight δ. The first-order condition with respect to the social activity changes to:

$$\frac{\partial U(x_{h,t}^I, x_{s,t}^I)}{\partial x_{s,t}^I} + \delta \beta \frac{\partial p_t(.)}{\partial x_{s,t}^I}(V_{t+1}^I - V_{t+1}^S) = 0. \tag{20}$$

Now the optimal level of social activity chosen by infected individuals is lower than the one obtained under (13) since they partly internalize the risk of infecting susceptible individuals, who then turn into infected ones next period. Time discounting is also relevant in this case: more patient individuals tend to internalize the impact of their social activity on the infection probability by more.

4.2. Extension to Networked SIR

Within communities there are different groups that have different exposure or contact rates to each of the other groups. Reciprocity in networks is the likelihood that two nodes (groups) are linked to each other.[19] Our empirical analysis has also uncovered a role for reciprocity. To capture such a role, we extend the SIR model to include different groups of the population that experience different contact rates. These groups could correspond to, e.g., the age

---

17 Warm-glow preferences have a long-standing tradition in economics. Besides Becker (1974)'s original work, see Andreoni (1989) or Andreoni (1993).
18 See, for instance, Bolton and Ockenfels (2000) or Andreoni and Miller (2002).
19 A more general concept of reciprocity can be found in Fehr and Schmidt (1999) or Fehr and Gächter (2000).

structure, different strengths in ties, or closer face-to-face interactions in the workplace. The underlying idea is that contact rates tend to be higher among peer groups.

Consider a population with different groups $j = 1, ..., J$. The number of people in each group is N_j. Groups have different probabilities of encounters with the others. The contact intensity between group j and any group k is $\xi_{j,k}$. Each susceptible individual of group j experiences a certain number of contacts per outings with infected individuals of his own but also of all the other groups. This number depends on the average level of social activity by the infected individuals of each group k weighted by the contact intensity across groups, and is equal to:

$$m^j(\bar{x}_{s,t}^j) = m^j(\bar{x}_{s,t}^{S,k}, \bar{x}_{s,t}^{I,k}) = m^j \left(\sum_k \xi_{j,k}(\bar{x}_{s,t}^{S,k} S_t^k + \bar{x}_{s,t}^{I,k} I_t^k) \right). \tag{21}$$

To obtain the average number of contacts between a susceptible person of group j and an infected individual from any group, we shall divide the total number of contacts by the average frequency of encounters between susceptible individuals in group j and infected individuals in any other group k. The latter is given by $\hat{x}_{s,t}^{S,j} = \bar{x}_{s,t}^{S,j} \sum_k \xi_{j,k} \bar{x}_{s,t}^{I,k}$. Therefore, the probability of infection of a susceptible person in group j is modified as follows:

$$p_t^j = x_{s,t}^{S,j} \left[\sum_k \eta \xi_{j,k} x_{s,t}^{I,k} \frac{m^j(\bar{x}_{s,t}^{S,k}, \bar{x}_{s,t}^{I,k})}{\hat{x}_{s,t}^{S,j}} I_t^k \right], \tag{22}$$

where $k = 1, .., J$ and $\xi_{j,j} = 1$. The underlying rationale is equivalent to the one described in the single-group case, except that now the probability of meeting an infected person from any other group k is weighted by the likelihood of the contacts $\xi_{j,k}$.

The SIR model for each group j then reads as follows:

$$S_{t+1}^j = S_t^j - x_{s,t}^{S,j} \left[\sum_k \eta \xi_{j,k} x_{s,t}^{I,k} \frac{m^j(\bar{x}_{s,t}^{S,k}, \bar{x}_{s,t}^{I,k})}{\hat{x}_{s,t}^{S,j}} I_t^k \right] S_t^j \tag{23}$$

$$I_{t+1}^j = I_t^j + x_{s,t}^{S,j} \left[\sum_k \eta \xi_{j,k} x_{s,t}^{I,k} \frac{m^j(\bar{x}_{s,t}^{S,k}, \bar{x}_{s,t}^{I,k})}{\hat{x}_{s,t}^{S,j}} I_t^k \right] S_t^j - \gamma I_t^j \tag{24}$$

$$R_{t+1}^j = R_t^j + \gamma I_t^j, \tag{25}$$

where $S_t + I_t + R_t \equiv 1$.

As before, atomistic individuals take the average social activity and the average social encounters as given. The first-order condition for social activity of the susceptible individuals belonging to group j now reads as follows:

$$\frac{\partial U(x_{h,t}^{S,j}, x_{s,t}^{S,j})}{\partial x_{s,t}^{S,j}} + \beta \left[\sum_k \eta \xi_{j,k} x_{s,t}^{I,k} \frac{m^j(\bar{x}_{s,t}^{S,k}, \bar{x}_{s,t}^{I,k})}{\hat{x}_{s,t}^{S,j}} I_t^k \right] (V_{t+1}^{I,j} - V_{t+1}^{S,j}) = 0. \tag{26}$$

Note that again, each susceptible agent takes the average level of social activity by the others as given. It becomes clear that the differential impact of her social activity on the various groups affects her optimal choice.

We can now derive the first-order conditions of the infected. For this purpose, we assume altruistic preferences, which means that the infected agents internalize at least partly, with the weight δ, the impact of their choices on the susceptible agents. The first-order condition with respect to social activity is:

$$\frac{\partial U(x_{h,t}^{I,j}, x_{s,t}^{I,j})}{\partial x_{s,t}^{I,j}} + \delta \beta x_{s,t}^{S,j} \eta \frac{m^j(\bar{x}_{s,t}^{S,j}, \bar{x}_{s,t}^{I,j})}{\hat{x}_{s,t}^{S,j}} I_t^j (V_{t+1}^{I,j} - V_{t+1}^{S,j}) = 0. \tag{27}$$

The first-order conditions for the recovered individuals are the same as in (14), but separately for each group j. We can now formulate an equilibrium definition of the decentralized SIR-network model.

Definition 2. A decentralized equilibrium for the SIR-network model is a sequence of state variables, S_t^j, I_t^j, R_t^j, a set of value functions, $V_t^{S,j}, V_t^{I,j}, V_t^{R,j}$, and a sequence of consumption, probabilities, and social contacts, $p_t^j, x_{h,t}^{S,j}, x_{h,t}^{I,j}, x_{h,t}^{R,j}, x_{s,t}^{S,j}, x_{s,t}^{I,j}, x_{s,t}^{R,j}$, such that:

1. S_t^j, I_t^j, R_t^j solve (16) to (18) for each group j, with the contact rate given by (22) for each group j

2. $V_t^{S,j}, V_t^{I,j}, V_t^{R,j}$ solve (6), (9), and (10), now defined separately for each group j

3. The sequence $p_t^j, x_{h,t}^{S,j}, x_{h,t}^{I,j}, x_{h,t}^{R,j}, x_{s,t}^{S,j}, x_{s,t}^{I,j}, x_{s,t}^{R,j}$ solves (26), (27) , (11), (13) and (14) for each group j.

4.3. Social Planner

As noted before, when each person chooses her optimal social activity, she does not consider its impact on the average level of social activity. We now introduce a social planner who takes this into account, starting with the planner problem for the homogeneous SIR model.

Social Planner in the Homogeneous SIR Model. The social planner chooses the consumption paths of home and social, i.e., outside, activities for each agent by maximizing the weighted sum of the utilities of all agents. The planner is aware that her policies affect the number of infected individuals in the following periods. Throughout this section, infected individuals hold altruistic preferences. The optimization problem is constrained by the SIR model, in which the contact probability is still given by (15). However, now the planner knows that in a symmetric Nash equilibrium all agents choose the same policy, hence she can set $x_{s,t}^S = \bar{x}_{s,t}^S$ and $x_{s,t}^I = \bar{x}_{s,t}^I$. Also, when choosing the social activity of each agent, she takes into account the impact on the matching function. Therefore, for the infection probability entering the SIR model, we can rewrite (15) as follows:

$$p_t^P = \eta m(x_{s,t}^S, x_{s,t}^I)I_t. \tag{28}$$

The planner chooses the sequence $[S_{t+1}, I_{t+1}, R_{t+1}, x_{h,t}^S, x_{h,t}^I, x_{h,t}^R, x_{s,t}^S, x_{s,t}^I, x_{s,t}^R]_{t=0}^{\infty}$ at any initial period t to maximize:

$$V_t^N = S_t V_t^S + I_t V_t^I + R_t V_t^R \tag{29}$$

subject to

$$S_{t+1} = S_t - \eta m(x_{s,t}^S, x_{s,t}^I)I_t S_t \tag{30}$$

$$I_{t+1} = I_t + \eta m(x_{s,t}^S, x_{s,t}^I)I_t S_t - \gamma I_t \tag{31}$$

$$R_{t+1} = R_t + \gamma I_t, \tag{32}$$

22

where $S_t + I_t + R_t \equiv 1$. The full set of first-order conditions can be found in Appendix B.

Proposition 1. The planner reduces social interactions on top and above the decentralized equilibrium. She does so due to a static and a dynamic externality.

Proof. The full set of first-order conditions of the constrained Pareto allocation is listed in Appendix B. The first-order conditions for home activities and for all activities of the recovered remain the same. However, after transforming (48) and (50) in Appendix B, the choices of the social activity of the susceptible and the infected agents now read as follows:

$$\frac{\partial U(x_{h,t}^S, x_{s,t}^S)}{\partial x_{s,t}^S} + \beta\eta\frac{\partial m(x_{s,t}^S, x_{s,t}^I)}{\partial x_{s,t}^S}I_t(1 + S_t)(V_{t+1}^I - V_{t+1}^S) = 0 \tag{33}$$

$$\frac{\partial U(x_{h,t}^I, x_{s,t}^I)}{\partial x_{s,t}^I} + \beta\eta\frac{\partial m(x_{s,t}^S, x_{s,t}^I)}{\partial x_{s,t}^I}I_t(\delta + S_t)(V_{t+1}^I - V_{t+1}^S) = 0. \tag{34}$$

Equations (33) and (34) are different from the first-order conditions for the optimal choice of social activity of susceptible and infected agents in the decentralized equilibrium (cf. equations (12) and (20)). The difference can be decomposed into two parts, which correspond to a static and a dynamic inefficiency. First, atomistic agents do not internalize the impact of their decisions on the average level of social activity, while the planner does. Given the functional form of the probability as per (15), this implies that in the decentralized equilibrium:

$$\frac{\partial p_t(.)}{\partial x_{s,t}^i} = \frac{p_t}{x_{s,t}^i} \text{ for } i = S, I, \tag{35}$$

i.e., susceptible and infected individuals, respectively. For the planner economy we have instead:

$$\frac{\partial p_t^P(.)}{\partial x_{s,t}^i} = \frac{\eta\partial m(x_{s,t}^S, x_{s,t}^I)I_t}{\partial x_{s,t}^i}. \tag{36}$$

Hence, the static inefficiency is given by:

$$\Phi_t^S = \beta \left(\frac{\eta \partial m(x_{s,t}^S, x_{s,t}^I) I_t}{\partial x_{s,t}^S} - \frac{p_t}{x_{s,t}^S} \right) (V_{t+1}^I - V_{t+1}^S) \tag{37}$$

$$\Phi_t^I = \beta \delta \left(\frac{\eta \partial m(x_{s,t}^S, x_{s,t}^I) I_t}{\partial x_{s,t}^I} - \frac{p_t}{x_{s,t}^I} \right) (V_{t+1}^I - V_{t+1}^S). \tag{38}$$

Note that the static inefficiency is affected by the matching function's returns to scale. In places with more dense interactions, the spread of the disease is faster and the size of the inefficiency is larger.

The second component that distinguishes (33) and (34) from (12) and (20) is:

$$\Psi_t^S = \beta \frac{\eta \partial m(x_{s,t}^S, x_{s,t}^I)}{\partial x_{s,t}^S} I_t S_t (V_{t+1}^I - V_{t+1}^S) \tag{39}$$

$$\Psi_t^I = \beta \frac{\eta \partial m(x_{s,t}^S, x_{s,t}^I)}{\partial x_{s,t}^I} I_t S_t (V_{t+1}^I - V_{t+1}^S). \tag{40}$$

This second component can be seen as a dynamic inefficiency: a planner acting under commitment can affect the future number of individuals in each state.

Social Planner in the SIR-Network Model. In the SIR-network model, the social planner maximizes the sum of future discounted utilities for all groups in the population taking as given the set of constraints, (23) to (25), for all groups in the population in which the equilibrium infection probabilities have been substituted. By symmetry of choices within each group, $x_{s,t}^{S,j} \sum_k \xi_{j,k} x_{s,t}^{I,k} = \bar{x}_{s,t}^{S,j} \sum_k \xi_{j,k} \bar{x}_{s,t}^{I,k}$, and the equilibrium infection probabilities for each group are now given by $p_t^{Pj} = \left[\sum_k \eta m^j(x_{s,t}^{S,k}, x_{s,t}^{I,k}) I_t^k \right]$.

Proposition 2. The inefficiencies in the SIR-network model are larger than in the homogeneous SIR model, and also take into account the reciprocal relations.

Proof. Given the above-noted definition of the social planner's problem for the SIR network, we can compute the first-order conditions of the planner problem. Comparing these with the

first-order conditions of the decentralized economy yields the following aggregate inefficiency for each group:

$$\chi_t^{S,j} = \beta \sum_{k \neq j} \eta \frac{\partial p_t^{Pk}}{\partial x_{s,t}^{S,j}}(1 + S_t^k)(V_{t+1}^{I,k} - V_{t+1}^{S,k}) + \beta \left(\frac{\partial p_t^{Pj}}{\partial x_{s,t}^{S,j}}(1 + S_t^j) - \frac{\partial p_t^j}{\partial x_{s,t}^{S,j}} \right)(V_{t+1}^{I,j} - V_{t+1}^{S,j}) \quad (41)$$

$$\chi_t^{I,j} = \beta \sum_{k \neq j} \eta \frac{\partial p_t^{Pk}}{\partial x_{s,t}^{I,j}}(\delta + S_t^k)(V_{t+1}^{I,k} - V_{t+1}^{S,k}) + \beta \left(\frac{\partial p_t^{Pj}}{\partial x_{s,t}^{I,j}}(\delta + S_t^j) - \delta\frac{\partial p_t^j}{\partial x_{s,t}^{I,j}} \right)(V_{t+1}^{I,j} - V_{t+1}^{S,j}), \quad (42)$$

where p_t^j takes the same functional form as in equation (22).

For the SIR-network model, the inefficiencies now include an additional component, the first term in (41) and (42), which depends on the reciprocity across groups. Now the planner internalizes not only the impact of the social activity of each group on the number of contacts within this group, but also how the reciprocity across groups affects total contacts.

Having characterized the inefficiencies, we next turn to actual implementation policies in the homogeneous SIR and the SIR-network model, and their suitability to close the inefficiencies.

4.4. Implementability: Partial Lockdown in the Homogeneous SIR Model and Targeted Lockdown in the SIR-Network Model

We now examine whether actual lockdown policies are efficient. In particular, we consider partial and targeted lockdown policies.

Partial Lockdown. We start by examining a simple partial lockdown policy for the homogeneous SIR model. We define as θ the fraction of social activity that is restricted. Note that the planner can enforce two different lockdown policies, θ^S and θ^I, only if there is the possibility to identify infected individuals. Let us first assume she cannot identify them and

there is only one single θ. Then, a partial lockdown policy affects the infection probability in the decentralized economy as follows:

$$p_t(\theta,.) = \eta x_{s,t}^S x_{s,t}^I \frac{m((1-\theta)\bar{x}_{s,t}^S, (1-\theta)\bar{x}_{s,t}^I)}{\bar{x}_{s,t}^S \bar{x}_{s,t}^I} I_t. \tag{43}$$

Lemma 1. The partial lockdown policy is efficient only in the presence of the means to identify infected individuals, such as universal testing.

Proof. The partial lockdown policy would be efficient if it set to zero the aggregate inefficiencies:

$$\beta \left[\eta \frac{\partial m(x_{s,t}^S, x_{s,t}^I)}{\partial x_{s,t}^S} I_t(1 + S_t) - \frac{p_t(\theta,.)}{x_{s,t}^S} \right] (V_{t+1}^I - V_{t+1}^S) = 0 \tag{44}$$

$$\beta \left[\eta \frac{\partial m(x_{s,t}^S, x_{s,t}^I)}{\partial x_{s,t}^I} I_t(\delta + S_t) - \delta \frac{p_t(\theta,.)}{x_{s,t}^I} \right] (V_{t+1}^I - V_{t+1}^S) = 0. \tag{45}$$

Equations (44) and (45) include both the static and the dynamic inefficiency. If the planner is endowed with a single instrument, i.e., a single lockdown policy applied equally to both susceptible and infected individuals, she cannot close these two inefficiencies. Only in presence of a second instrument, specifically a measure to identify infected individuals, she can target policies toward agents in these two states and set the inefficiencies to zero.

Targeted Lockdown Policies. We have seen that in the SIR-network model, a number j of inefficiencies for both the susceptible and the infected individuals arise, as summarized in equations (41) and (42). The result from Lemma 1 extends here as well. The planner could design lockdown policies differentiated across groups according to the parameters θ_j^S and θ_j^I. However, she could do so only in the presence of the means to identify infected individuals in each group.

5. Concluding Remarks

While envisaging a return to freedom of mobility and to past customs, though hopefully with fading fears, understanding the determinants of people's behavior in the face of catastrophic events is important along at least two dimensions. First, it is difficult to accurately forecast the spread of a disease with models that do not account for human behavior. Second, as policymakers seek advice on exit strategies that could mitigate both the loss of lives and the economic consequences, understanding individuals' behavior even as lockdowns or other stringency measures are lifted is informative. Excessive precautionary behavior is likely to trigger demand spirals which might slow down the recovery process.

We use daily mobility data for 89 cities worldwide to show that preference traits, such as patience and altruism, and community traits, such as reciprocity, matter for the behavioral response of individuals during a pandemic. We rationalize this behavior by proposing extensions of the homogeneous SIR and the SIR-network model that account for agents' optimizing behavior.

One of the initial approaches to contain the pandemic, suggested by experts, has been a "one size fits all" response, namely a full lockdown. We uncover important heterogeneities in individuals' behavior as well as in the efficacy of stringency measures with respect to regional differences in time and social preferences. Our findings suggest that a balanced approach involving a joint interaction of stringency measures, in respect of human dignity, and responsible social preferences can help mitigate both the public health crisis and the economic costs. Finally, by designing the planner problems, we show that a static and a dynamic inefficiency arise in the homogeneous SIR model, and a reciprocity inefficiency in the SIR-network model. However the planner can close those inefficiencies only if targeted lockdown policies are accompanied by the possibility to identify infected individuals.

References

Acemoglu, D., Chernozhukov, V., Werning, I., and Whinston, M. D. (2020). A Multi-Risk SIR Model with Optimally Targeted Lockdown. *NBER Working Paper No. 27102*.

Alvarez, F., Argente, D., and Lippi, F. (2020). A Simple Planning Problem for COVID-19 Lockdown. *CEPR Discussion Paper No. 14658*.

Ambrus, A., Mobius, M., and Szeidl, A. (2014). Consumption Risk-Sharing in Social Networks. *American Economic Review*, 1(104):149–182.

Andreoni, J. (1989). Giving with Impure Altruism: Applications to Charity and Ricardian Equivalence. *Journal of Political Economy*, 97(6):1447–1458.

Andreoni, J. (1993). An Experimental Test of the Public Goods Crowding-Out Hypothesis. *American Economic Review*, 83(5):1317–1327.

Andreoni, J. and Miller, J. (2002). Giving according to GARP: An Experimental Test of the Consistency of Preferences for Altruism. *Econometrica*, 70(2):737–753.

Atkenson, A. (2020). What Will Be the Economic Impact of COVID-19 in the US? Rough Estimates of Disease Scenarios. *NBER Working Paper No. 26868*.

Bartik, A. W., Bertrand, M., Cullen, Z. B., Glaeser, E. L., Luca, M., and Stanton, C. T. (2020). How Are Small Businesses Adjusting to COVID-19? Early Evidence from a Survey. *NBER Working Paper No. 26989*.

Becker, G. (1974). A Theory of Social Interactions. *Journal of Political Economy*, 82(6):1063–1083.

Bloch, F., Génicot, G., and Ray, D. (2008). Informal Insurance in Social Networks. *Journal of Economic Theory*, 1(143):36–58.

Bolton, G. E. and Ockenfels, A. (2000). ERC: A Theory of Equity, Reciprocity, and Competition. *American Economic Review*, 90(2):166–193.

Bramoulle, Y. and Kranton, R. (2007). Risk-Sharing Networks. *Journal of Economic Behavior & Organization*, 3-4(64):275–294.

Colizza, V., Pastor-Satorras, R., and Vespigiani, A. (2007). Reaction–Diffusion Processes and Metapopulation Models in Heterogeneous Networks. *Nature Physics*, (3):276–282.

Coven, J. and Gupta, A. (2020). Disparities in Mobility Responses to COVID-19. *NYU Stern Working Paper*.

Diamond, P. A. (1982). Aggregate Demand Management in Search Equilibrium. *Journal of Political Economy*, 90(5):881–894.

Durante, R., Guiso, L., and Gulino, G. (2020). Civic Capital and Social Distancing: Evidence from Italians' Response to COVID-19. *Universitat Pompeu Fabra Working Paper*.

Eichenbaum, M., Rebelo, S., and Trabandt, M. (2020). The Macroeconomics of Epidemics. *CEPR Discussion Paper No. 14520*.

Falk, A., Becker, A., Dohmen, T., Enke, B., Huffman, D., and Sunde, U. (2018). Global Evidence on Economic Preferences. *Quarterly Journal of Economics*, 133(4):1645–1692.

Falk, A., Becker, A., Dohmen, T., Huffman, D., and Sunde, U. (2016). The Preference Survey Module: A Validated Instrument for Measuring Risk, Time, and Social Preferences. *IZA Discussion Paper No. 9674*.

Farboodi, M., Jarosch, G., and Shimer, R. (2020). Externality of Social Distancing. *Covid Economics: Vetted and Real-Time Papers*, 9.

Fehr, E. and Gächter, S. (2000). Fairness and Retaliation: The Economics of Reciprocity. *Journal of Economic Perspectives*, 3(14):159–181.

Fehr, E. and Schmidt, K. (1999). A Theory of Fairness, Competition and Cooperation. *Quarterly Journal of Economics*, 3(114):817–868.

Garibaldi, P., Moen, E., and Pissarides, C. (2020). Modelling Contacts and Transitions in the SIR Epidemics Model. *Covid Economics: Vetted and Real-Time Papers*, 5.

Glover, A., Heathcote, J., Krueger, D., and Ríos-Rull, J. V. (2020). Health versus Wealth: On the Distributional Effects of Controlling a Pandemic. *Covid Economics: Vetted and Real-Time Papers*, 6.

Hethcote, H. (2000). The Mathematics of Infectious Diseases. *SIAM Review*, 42(4):599–653.

Kaplan, G., Moll, B., and Violante, G. (2020). Pandemics According to HANK. *Princeton University Working Paper*.

Kermack, O. and McKendrick, A. G. (1927). Contributions to the Mathematical Theory of Epidemics. *Proceedings Royal Society London*, (115):700–721.

Krueger, D., Uhlig, H., and Xie, T. (2020). Macroeconomic Dynamics and Reallocation in an Epidemic. *CEPR Discussion Paper No. 14607*.

Moinet, A., Pastor-Satorras, R., and Barrat, A. (2018). Effect of Risk Perception on Epidemic Spreading in Temporal NetworkS. *Physical Review*, 97(1).

Moser, C. A. and Yared, P. (2020). Pandemic Lockdown: The Role of Government Commitment. *NBER Working Paper No. 27062*.

Pastor-Satorras, R. and Vespigiani, A. (2000). Epidemic Dynamics and Endemic States in Complex Networks. *Physical Review*, 6(63):276–282.

Pastor-Satorras, R. and Vespigiani, A. (2001). Epidemic Spreading in Scale-Free Networks. *Physical Review Letters*, 86(14):276–282.

Perra, N., Gonçalves, B., Pastor-Satorras, R., and Vespigiani, A. (2018). Activity Driven Modeling of Time Varying Networks. *Scientific Reports, Nature*, 2(469).

Petrongolo, B. and Pissarides, C. A. (2001). Looking into the Black Box: A Survey of the Matching Function. *Journal of Economic Literature*, 39(2):390–431.

Pissarides, C. A. (2000). *Equilibrium Unemployment Theory*. The MIT Press, 2nd edition.

A. Tables

Table 1
Summary Statistics

	Country level				City/regional level			
	Mean	Std. dev.	Min	Max	Mean	Std. dev.	Min	Max
Walking	85.17	42.89	3.78	324.06	86.04	43.31	3.78	324.06
Driving	82.01	35.23	7.52	195.53	82.25	35.48	7.52	194.74
Transit	76.53	44.09	4.11	322.18	77.21	45.18	4.11	322.18
Corona ST	31.63	25.34	1.00	100.00	31.93	25.70	0.00	100.00
Stringency index	38.44	34.19	0.00	100.00				
Patience					0.57	0.42	-0.47	1.42
Altruism					0.12	0.30	-0.98	0.60
Neg. reciprocity					0.05	0.25	-0.45	0.57
N	8,099				5,460			

This table presents summary statistics for the main dependent and independent variables, which correspond to the respective descriptions in Tables 2 to 6. The statistics in the first four columns are at the country-day level, whereas the statistics in the last four columns are at the city-day level for the three mobility outcomes (walking, driving, and transit) and at the region-day level for all remaining variables. Furthermore, the sample in the last four columns is limited to countries with at least two cities in different regions.

Table 2
Effect of Fear and Government Responses on Mobility

Variable	ln(Walking) (1)	ln(Driving) (2)	ln(Transit) (3)	ln(Walking) (4)	ln(Driving) (5)	ln(Transit) (6)
ln(Corona ST_{t-1})	-0.152**	-0.166***	-0.131*	-0.113**	-0.134***	-0.084
	(0.057)	(0.052)	(0.073)	(0.050)	(0.048)	(0.061)
Lockdown	-0.394***	-0.338***	-0.276			
	(0.125)	(0.111)	(0.187)			
Stringency index				-0.005***	-0.004***	-0.006***
				(0.001)	(0.001)	(0.002)
Cases per capita$_{t-1}$	-0.057	0.010	-0.108	-0.108	-0.034	-0.120
	(0.143)	(0.113)	(0.133)	(0.141)	(0.107)	(0.124)
City FE	Y	Y	Y	Y	Y	Y
Date FE	Y	Y	Y	Y	Y	Y
Adj. R^2	0.81	0.82	0.86	0.80	0.81	0.86
N	7,740	7,740	5,580	7,740	7,740	5,580

The level of observation is the city-date level it, where city i is in region g of country c. The dependent variable in columns 1 and 4 is the natural logarithm of Apple Mobility's walking index for city i at date t. The dependent variable in columns 2 and 5 is the natural logarithm of Apple Mobility's driving index for city i at date t. The dependent variable in columns 3 and 6 is the natural logarithm of Apple Mobility's transit index for city i at date t. Corona ST_{ct-1} is the Google Trends Index for the search term "Coronavirus" in country c at date $t-1$. Lockdown$_{ct}$ is an indicator variable for the lockdown period in country c (or state/region g for the US) at date t. Stringency index$_{ct}$ is the stringency index (taken from the Oxford COVID-19 Government Response Tracker), reflecting the different policy responses that governments have taken, in country c at date t. Cases per capita$_{ct-1}$ are the infection cases per capita in country c at date $t-1$, and are multiplied by 1,000. Robust standard errors (double-clustered at the city and date levels) are in parentheses.

Table 3

Effect of Fear and Government Responses on Mobility – Regional-level Variation

Variable	ln(Walking) (1)	ln(Driving) (2)	ln(Transit) (3)	ln(Walking) (4)	ln(Driving) (5)	ln(Transit) (6)
$\ln(\text{Corona ST}_{t-1})$	-0.176***	-0.177***	-0.072	-0.109***	-0.120***	-0.012
	(0.040)	(0.038)	(0.050)	(0.038)	(0.038)	(0.046)
Lockdown	-0.414***	-0.365***	-0.186			
	(0.109)	(0.089)	(0.134)			
Stringency index				-0.007***	-0.006***	-0.007***
				(0.001)	(0.001)	(0.001)
Cases per capita$_{t-1}$	-0.137	-0.047	-0.173	-0.180	-0.085	-0.146
	(0.118)	(0.095)	(0.104)	(0.116)	(0.089)	(0.107)
City FE	Y	Y	Y	Y	Y	Y
Date FE	Y	Y	Y	Y	Y	Y
Adj. R^2	0.80	0.82	0.84	0.80	0.81	0.85
N	5,393	5,393	4,404	5,393	5,393	4,404

The level of observation is the city-date level it, where city i is in region g of country c. The sample is limited to countries c with at least two cities i in different regions g. The dependent variable in columns 1 and 4 is the natural logarithm of Apple Mobility's walking index for city i at date t. The dependent variable in columns 2 and 5 is the natural logarithm of Apple Mobility's driving index for city i at date t. The dependent variable in columns 3 and 6 is the natural logarithm of Apple Mobility's transit index for city i at date t. *Corona* ST_{gt-1} is the Google Trends Index for the search term "Coronavirus" in region g at date $t-1$. *Lockdown$_{ct}$* is an indicator variable for the lockdown period in country c (or state/region g for the US) at date t. *Stringency index$_{ct}$* is the stringency index (taken from the Oxford COVID-19 Government Response Tracker), reflecting the different policy responses that governments have taken, in country c at date t. *Cases per capita$_{ct-1}$* are the infection cases per capita in country c at date $t-1$, and are multiplied by 1,000. Robust standard errors (double-clustered at the city and date levels) are in parentheses.

Table 4

Table 4
Effect of Fear and Government Responses on Mobility: The Role of Patience – Regional-level Variation

Variable	ln(Walking) (1)	ln(Driving) (2)	ln(Transit) (3)	ln(Walking) (4)	ln(Driving) (5)	ln(Transit) (6)
ln(Corona ST_{t-1})	-0.024	-0.034**	0.025	0.049*	0.022	0.122***
	(0.025)	(0.017)	(0.035)	(0.026)	(0.021)	(0.030)
Lockdown	-0.927***	-0.815***	-0.823***			
	(0.155)	(0.112)	(0.221)			
Lockdown	0.760***	0.691***	0.596**			
$\times$ Patience	(0.179)	(0.122)	(0.268)			
Stringency index				-0.007***	-0.006***	-0.009***
				(0.002)	(0.001)	(0.003)
Stringency index				0.006***	0.004***	0.005*
$\times$ Patience				(0.001)	(0.001)	(0.003)
Cases per capita$_{t-1}$	-0.150	-0.061	-0.149	-0.119	-0.035	-0.066
	(0.093)	(0.065)	(0.102)	(0.122)	(0.091)	(0.115)
City FE	Y	Y	Y	Y	Y	Y
Date FE	Y	Y	Y	Y	Y	Y
Country-month FE	Y	Y	Y	Y	Y	Y
Adj. R^2	0.91	0.93	0.92	0.90	0.91	0.91
N	5,393	5,393	4,404	5,393	5,393	4,404

The level of observation is the city-date level it, where city i is in region g of country c. The sample is limited to countries c with at least two cities i in different regions g. The dependent variable in columns 1 and 4 is the natural logarithm of Apple Mobility's walking index for city i at date t. The dependent variable in columns 2 and 5 is the natural logarithm of Apple Mobility's driving index for city i at date t. The dependent variable in columns 3 and 6 is the natural logarithm of Apple Mobility's transit index for city i at date t. Corona ST_{gt-1} is the Google Trends Index for the search term "Coronavirus" in region g at date $t-1$. Lockdown$_{ct}$ is an indicator variable for the lockdown period in country c (or state/region g for the US) at date t. Stringency index$_{ct}$ is the stringency index (taken from the Oxford COVID-19 Government Response Tracker), reflecting the different policy responses that governments have taken, in country c at date t. Patience$_g$ is the average value for the measure of time preference in region g reported by Falk et al. (2018). Cases per capita$_{ct-1}$ are the infection cases per capita in country c at date $t-1$, and are multiplied by 1,000. Robust standard errors (double-clustered at the city and date levels) are in parentheses.

Table 5
Effect of Fear and Government Responses on Mobility: The Role of Negative Reciprocity − Regional-level Variation

Variable	ln(Walking) (1)	ln(Driving) (2)	ln(Transit) (3)	ln(Walking) (4)	ln(Driving) (5)	ln(Transit) (6)
ln(Corona ST$_{t-1}$)	-0.037	-0.046**	0.017	0.021	0.004	0.083***
	(0.027)	(0.020)	(0.035)	(0.029)	(0.022)	(0.031)
Lockdown	-0.424***	-0.359***	-0.349***			
	(0.093)	(0.075)	(0.101)			
Lockdown	-0.583**	-0.510***	-0.917***			
× Neg. reciprocity	(0.225)	(0.167)	(0.271)			
Stringency index				-0.004***	-0.003***	-0.005***
				(0.001)	(0.001)	(0.002)
Stringency index				-0.001	-0.002	-0.007**
× Neg. reciprocity				(0.002)	(0.002)	(0.003)
Cases per capita$_{t-1}$	-0.132	-0.045	-0.144	-0.138	-0.048	-0.086
	(0.104)	(0.076)	(0.110)	(0.125)	(0.092)	(0.123)
City FE	Y	Y	Y	Y	Y	Y
Date FE	Y	Y	Y	Y	Y	Y
Country-month FE	Y	Y	Y	Y	Y	Y
Adj. R^2	0.90	0.92	0.92	0.89	0.91	0.91
N	5,393	5,393	4,404	5,393	5,393	4,404

The level of observation is the city-date level it, where city i is in region g of country c. The sample is limited to countries c with at least two cities i in different regions g. The dependent variable in columns 1 and 4 is the natural logarithm of Apple Mobility's walking index for city i at date t. The dependent variable in columns 2 and 5 is the natural logarithm of Apple Mobility's driving index for city i at date t. The dependent variable in columns 3 and 6 is the natural logarithm of Apple Mobility's transit index for city i at date t. Corona ST_{gt-1} is the Google Trends Index for the search term "Coronavirus" in region g at date $t-1$. Lockdown$_{ct}$ is an indicator variable for the lockdown period in country c (or state/region g for the US) at date t. Stringency index$_{ct}$ is the stringency index (taken from the Oxford COVID-19 Government Response Tracker), reflecting the different policy responses that governments have taken, in country c at date t. Neg. reciprocity$_g$ is the average value for the measure of negative reciprocity in region g reported by Falk et al. (2018). Cases per capita$_{ct-1}$ are the infection cases per capita in country c at date $t-1$, and are multiplied by 1,000. Robust standard errors (double-clustered at the city and date levels) are in parentheses.

Table 6
Effect of Fear and Government Responses on Mobility: The Role of Altruism –
Regional-level Variation

Variable	ln(Walking) (1)	ln(Driving) (2)	ln(Transit) (3)	ln(Walking) (4)	ln(Driving) (5)	ln(Transit) (6)
ln(Corona ST$_{t-1}$)	-0.041	-0.048**	0.013	0.019	0.003	0.089***
	(0.027)	(0.021)	(0.035)	(0.030)	(0.023)	(0.032)
Lockdown	-0.537***	-0.448***	-0.517***			
	(0.101)	(0.081)	(0.111)			
Lockdown	0.539**	0.395**	0.674**			
× Altruism	(0.217)	(0.154)	(0.281)			
Stringency index				-0.004***	-0.003***	-0.005***
				(0.001)	(0.001)	(0.002)
Stringency index				0.003	0.002	0.004
× Altruism				(0.002)	(0.001)	(0.003)
Cases per capita$_{t-1}$	-0.143	-0.053	-0.153	-0.135	-0.046	-0.082
	(0.107)	(0.079)	(0.113)	(0.124)	(0.092)	(0.123)
City FE	Y	Y	Y	Y	Y	Y
Date FE	Y	Y	Y	Y	Y	Y
Country-month FE	Y	Y	Y	Y	Y	Y
Adj. R^2	0.90	0.92	0.92	0.89	0.91	0.91
N	5,393	5,393	4,404	5,393	5,393	4,404

The level of observation is the city-date level it, where city i is in region g of country c. The sample is limited to countries c with at least two cities i in different regions g. The dependent variable in columns 1 and 4 is the natural logarithm of Apple Mobility's walking index for city i at date t. The dependent variable in columns 2 and 5 is the natural logarithm of Apple Mobility's driving index for city i at date t. The dependent variable in columns 3 and 6 is the natural logarithm of Apple Mobility's transit index for city i at date t. *Corona* ST_{gt-1} is the Google Trends Index for the search term "Coronavirus" in region g at date $t-1$. *Lockdown*$_{ct}$ is an indicator variable for the lockdown period in country c (or state/region g for the US) at date t. *Stringency index*$_{ct}$ is the stringency index (taken from the Oxford COVID-19 Government Response Tracker), reflecting the different policy responses that governments have taken, in country c at date t. *Altruism*$_g$ is the average value for the measure of altruism in region g reported by Falk et al. (2018). *Cases per capita*$_{ct-1}$ are the infection cases per capita in country c at date $t-1$, and are multiplied by 1,000. Robust standard errors (double-clustered at the city and date levels) are in parentheses.

B. Social Planner First-Order Conditions

For simplicity, we will normalize N_t to 1. Define as $\lambda_t^S, \lambda_t^I, \lambda_t^R$ the lagrange multipliers on equations (16) to (18). The set of first-order conditions with respect to the variables $S_{t+1}, I_{t+1}, R_{t+1}, x_{h,t}^S, x_{h,t}^I, x_{h,t}^R, x_{s,t}^S, x_{s,t}^I, x_{s,t}^R$ are:

$$\beta V_{t+1}^S = \lambda_t^S, \beta V_{t+1}^I = \lambda_t^I, \beta V_{t+1}^R = \lambda_t^R \tag{46}$$

$$\frac{\partial U(x_{h,t}^S, x_{s,t}^S)}{\partial x_{h,t}^S} = 0 \tag{47}$$

$$\frac{\partial U(x_{h,t}^S, x_{s,t}^S)}{\partial x_{s,t}^S} + \beta \frac{\partial p_t^P(.)}{\partial x_{s,t}^S}(V_{t+1}^I - V_{t+1}^S) - \lambda_t^S \frac{\partial p_t^P(.)}{\partial x_{s,t}^S} S_t + \lambda_t^I \frac{\partial p_t^P(.)}{\partial x_{s,t}^S} S_t = 0 \tag{48}$$

$$\frac{\partial U(x_{h,t}^I, x_{s,t}^I)}{\partial x_{h,t}^I} = 0 \tag{49}$$

$$\frac{\partial U(x_{h,t}^I, x_{s,t}^I)}{\partial x_{s,t}^I} - \lambda_t^S \frac{\partial p_t^P(.)}{\partial x_{s,t}^I} S_t + \lambda_t^I \frac{\partial p_t^P(.)}{\partial x_{s,t}^I} S_t = 0 \tag{50}$$

$$\frac{\partial U(x_{h,t}^R, x_{s,t}^R)}{\partial x_{h,t}^R} = 0; \frac{\partial U(x_{h,t}^R, x_{s,t}^R)}{\partial x_{s,t}^R} = 0 \tag{51}$$

with

$$\frac{\partial p_t^P(.)}{\partial x_{s,t}^S} = \eta \frac{\partial m(x_{s,t}^S, x_{s,t}^I)}{\partial x_{s,t}^S} I_t \text{ and } \frac{\partial p_t^P(.)}{\partial x_{s,t}^I} = \eta \frac{\partial m(x_{s,t}^S, x_{s,t}^I)}{\partial x_{s,t}^I} I_t. \tag{52}$$

Since $\lambda_t^I - \lambda_t^S = \beta(V_{t+1}^I - V_{t+1}^S)$, (48) and (50) become, respectively:

$$\frac{\partial U(x_{h,t}^S, x_{s,t}^S)}{\partial x_{s,t}^S} + \beta \eta \frac{\partial m(x_{s,t}^S, x_{s,t}^I)}{\partial x_{s,t}^S} I_t(1 + S_t)(V_{t+1}^I - V_{t+1}^S) = 0 \tag{53}$$

$$\frac{\partial U(x_{h,t}^I, x_{s,t}^I)}{\partial x_{s,t}^I} + \beta \eta \frac{\partial m(x_{s,t}^S, x_{s,t}^I)}{\partial x_{s,t}^I} I_t(\delta + S_t)(V_{t+1}^I - V_{t+1}^S) = 0. \tag{54}$$